Journal of the Mechanics and Physics of Solids 58 (2010) 860–873

Contents lists available at ScienceDirect

Journal of the Mechanics and Physics of Solids

journal homepage: www.elsevier.com/locate/jmps

Constitutive analysis of thin biological membranes with application to radial stretching of a hollow circular membrane

V.A. Lubarda *

Department of Mechanical and Aerospace Engineering, University of California, San Diego; La Jolla, CA 92093-0411, USA

ARTICLE INFO

Article history:
Received 26 November 2009
Received in revised form
18 March 2010
Accepted 31 March 2010

Keywords:
Membrane
Nonlinear elasticity
Red blood cell
Tension field
Wrinkling

ABSTRACT

The constitutive analysis of the mechanical response of thin elastic membranes under inplane deformation is presented by using the multiplicative decomposition of the deformation gradient into its areal and distortional parts. Specific results are obtained for the Evans–Skalak form of the strain energy function. The solution to the problem of radial stretching of a hollow circular membrane obeying this constitutive model is then derived. The stress concentration factor is determined as a function of the relative hole size and the magnitude of the applied tension. The tension boundary is identified above which no compressive stress appears in the membrane. The limit boundary is introduced below which the membrane cannot support the applied loading without unstable wrinkling. For the loading between the tension and the limit boundary, nonuniformly distributed infinitesimal wrinkles appear within the inner portion of the membrane, carrying radial tension but no circumferential stress (tension field). The specific form of the strain energy function is used to describe this behavior, and to calculate the amount of the membrane area absorbed by infinitesimal wrinkles. The wrinkled portion is surrounded by the outer portion of the membrane carrying both radial and circumferential stresses. The limit boundary is reached when wrinkles spread throughout the membrane. It is shown that for a sufficiently large tension at the outer boundary, the wrinkling does not spread throughout the membrane no matter how large the applied tension at the inner boundary of the membrane is, provided that no rupture takes place. The limiting extent of the tension field in such cases is calculated. The linearized version of the analysis is characterized by a closed form solution.

1. Introduction

A thin membrane is considered whose thickness is so small that the model of the continuum mechanics applies only within the plane of the membrane. Because of its negligible thickness, applied forces are considered to be distributed along the length, so that the membrane stresses are defined by the force/length ratios,[1] having the dimension N/m. Since an infinitesimally thin membrane has no buckling resistance, the membrane loading is assumed to be such that the principal membrane stresses are noncompressive. This continuum model can be used to study some aspects of the mechanical behavior of thin biological membranes, such as red blood cells (Evans and Skalak, 1980; Fung, 1993; Boal, 2002). More sophisticated bio-chemo-mechanical models, which include dynamic reorganization and active remodeling of cell during

* Tel.: +1 858 534 3169; fax: +1 858 534 5698.
E-mail address: vlubarda@ucsd.edu

[1] For example, the thickness of a red blood cell is about 50–100 Å, while its diameter and height (in its equilibrium biconcave shape) are about 8 μm and 2−3 μm, respectively.

0022-5096/$ - see front matter © 2010 Elsevier Ltd. All rights reserved.
doi:10.1016/j.jmps.2010.03.008

its large deformation, are needed to explain other aspects of the cell behavior (Gov, 2007; Li et al., 2007; Park et al., 2010). This is beyond the scope of the present analysis, although it could be pursued at the phenomenological level by extending the related work on constitutive theory of biological remodeling and growth (Lubarda and Hoger, 2002; Garikipati et al., 2006; Dervaux et al., 2009; Taber, 2009).

In this paper, we present the constitutive analysis of thin elastic membranes under large inplane deformations by using the multiplicative decomposition of the deformation gradient into its areal and distortional parts. The deformation parameters (ζ,Γ) are used to account for the two distinct modes of deformation. The strain energy is expressed as the sum of the contributions from the areal change (represented by the parameter ζ), and the distortional deformation (represented by the parameter Γ). The corresponding decomposition of the stress is established. Specific results are obtained for the Evans–Skalak form of the strain energy function. The solution to the problem of the radial stretching of a hollow circular membrane obeying this constitutive model is then derived. The stress concentration factor is determined as a function of the relative hole size and the magnitude of the applied tension. The tension boundary is identified above which no compressive stress appears in the membrane. For the loadings below the tension boundary, the membrane will wrinkle due to the lack of compressive (buckling) strength. We analyze early stages of wrinkling by assuming that wrinkles are infinitesimal and continuously but nonuniformly distributed within the inner portion of the membrane, which carries radial tension but no circumferential stress. This is known as a tension field analysis (Pipkin, 1986; Steigmann, 1990; Haughton, 2001). The specific form of the strain energy function is proposed and used to describe this behavior, and to calculate the amount of the membrane area absorbed by infinitesimal wrinkles. The inner tension-field portion is surrounded by the outer portion of the membrane, which carries both radial and circumferential stresses. With the further increase of loading, infinitesimal wrinkles may spread throughout the membrane. We refer to this limiting state as the limit boundary state. The membrane cannot support the loading states below the limit boundary without unstable wrinkling. The analysis of unstable wrinkling and the determination of the shape and discrete distribution of finite wrinkles is beyond the membrane theory, and requires the incorporation of the bending stiffness of the membrane. It is shown that for a sufficiently large tension at the outer boundary, the membrane will not reach the limit boundary state no matter how large the applied tension at the inner boundary of the membrane is, provided that no rupture takes place. The limiting extent of the tension field in such cases is then calculated. The analysis is performed for the prescribed traction and for the two types of mixed boundary conditions, with full details given in the case of the traction boundary conditions. The linearized version of the analysis, applicable to small strains, yields the closed form expressions for the tension and limit boundaries, and for the stress and displacement fields.

2. Kinematics of deformation

Consider an inplane deformation of a thin membrane element, with the principal stretches λ_1 and λ_2. The corresponding deformation gradient is $\mathbf{F}=\lambda_1\mathbf{n}_1\mathbf{N}_1+\lambda_2\mathbf{n}_2\mathbf{N}_2$, where $\mathbf{N}_i$ are the unit vectors along the principal directions of the stretch tensor $\mathbf{U}$ in the undeformed configuration, and $\mathbf{n}_i=\mathbf{R}\cdot\mathbf{N}_i$ are the unit vectors in the deformed configuration, along the principal directions of the stretch tensor $\mathbf{V}$. The inplane rotation tensor $\mathbf{R}=\mathbf{n}_1\mathbf{N}_1+\mathbf{n}_2\mathbf{N}_2$ relates $\mathbf{U}$ and $\mathbf{V}$ by the polar decomposition $\mathbf{F}=\mathbf{V}\cdot\mathbf{R}=\mathbf{R}\cdot\mathbf{U}$.

Imagine that the total deformation is achieved in two steps: by a purely distortional (isoareal) deformation, accompanied by the rotation, followed by the deformation which changes the membrane area only (Fig. 1). The deformation gradient can be accordingly decomposed as $\mathbf{F}=\mathbf{F}_{\mathrm{a}}\cdot\mathbf{F}_{\mathrm{d}}$, where

$$\mathbf{F}_{\mathrm{a}}=\lambda_{\mathrm{a}}(\mathbf{n}_1\mathbf{n}_1+\mathbf{n}_2\mathbf{n}_2),\quad \mathbf{F}_{\mathrm{d}}=\lambda_{\mathrm{d}}\mathbf{n}_1\mathbf{N}_1+\frac{1}{\lambda_{\mathrm{d}}}\mathbf{n}_2\mathbf{N}_2. \tag{1}$$

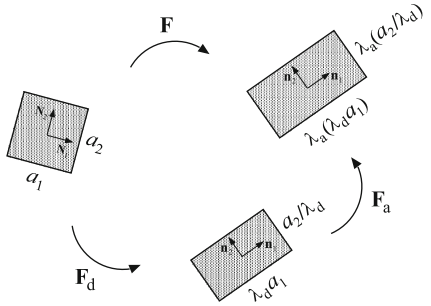

Fig. 1. The schematics of the multiplicative decomposition of the deformation gradient $\mathbf{F}$ into its areal and distortional parts. The rectangular element is subjected to distortional deformation with the stretch ratios λ_{d} and $1/\lambda_{\mathrm{d}}$ and the rotation, followed by an isotropic areal change with the stretch ratio λ_{a}.

Thus, $\lambda_a\lambda_d=\lambda_1$ and $\lambda_a/\lambda_d=\lambda_2$, which can be solved to λ_a and λ_d to obtain $\lambda_a=(\lambda_1\lambda_2)^{1/2}$ and $\lambda_d=(\lambda_1/\lambda_2)^{1/2}$. The areal and deviatoric parts of the multiplicative decomposition of the deformation gradient can therefore be expressed as

$$\mathbf{F}_a=\sqrt{\lambda_1\lambda_2}(\mathbf{n}_1\mathbf{n}_1+\mathbf{n}_2\mathbf{n}_2),\quad \mathbf{F}_d=\frac{1}{\sqrt{\lambda_1\lambda_2}}(\lambda_1\mathbf{n}_1\mathbf{N}_1+\lambda_2\mathbf{n}_2\mathbf{N}_2). \tag{2}$$

The Lagrangian and Eulerian strains are defined by $\mathbf{E}=(\mathbf{U}^2-\boldsymbol{\delta})/2$ and $\mathbf{e}=(\boldsymbol{\delta}-\mathbf{V}^{-2})/2$, where $\boldsymbol{\delta}$ is the unit tensor. It readily follows that

$$\mathbf{E}=\mathbf{E}_a+\lambda_a^2\mathbf{E}_d,\quad \mathbf{e}=\mathbf{e}_a+\frac{1}{\lambda_a^2}\mathbf{e}_d, \tag{3}$$

where

$$\mathbf{E}_a=\tfrac{1}{2}(\lambda_a^2-1)\boldsymbol{\delta},\quad \mathbf{e}_a=\tfrac{1}{2}(1-\lambda_a^{-2})\boldsymbol{\delta}, \tag{4}$$

and

$$\mathbf{E}_d=\tfrac{1}{2}(\lambda_d^2-1)\mathbf{N}_1\mathbf{N}_1+\tfrac{1}{2}(\lambda_d^{-2}-1)\mathbf{N}_2\mathbf{N}_2,$$

$$\mathbf{e}_d=\tfrac{1}{2}(1-\lambda_d^{-2})\mathbf{n}_1\mathbf{n}_1+\tfrac{1}{2}(1-\lambda_d^2)\mathbf{n}_2\mathbf{n}_2. \tag{5}$$

The traces of $\mathbf{E}_a$ and $\mathbf{e}_a$ are

$$\operatorname{tr}\mathbf{E}_a=\lambda_a^2-1=\lambda_1\lambda_2-1,\quad \operatorname{tr}\mathbf{e}_a=1-\lambda_a^{-2}=\frac{\lambda_1\lambda_2-1}{\lambda_1\lambda_2}. \tag{6}$$

Thus, $\operatorname{tr}\mathbf{E}_a$ is equal to the area change per unit undeformed area, while $\operatorname{tr}\mathbf{e}_a$ is equal to the area change per unit deformed area. Similarly,

$$\operatorname{tr}\mathbf{E}_d=\frac{1}{2}(\lambda_d^2+\lambda_d^{-2})-1=\frac{1}{2}\left(\frac{\lambda_1}{\lambda_2}+\frac{\lambda_2}{\lambda_1}\right)-1,$$

$$\operatorname{tr}\mathbf{e}_d=1-\frac{1}{2}(\lambda_d^2+\lambda_d^{-2})=-\operatorname{tr}\mathbf{E}_d. \tag{7}$$

The deformation parameter $\Gamma=\operatorname{tr}\mathbf{E}_d$ represents a symmetric (arithmetic mean) measure of the aspect ratio change (Evans and Skalak, 1980). This parameter can also be expressed in terms of the angles ϕ and ψ (Fig. 2a) as

$$\Gamma=\frac{1}{2}\left(\tan\frac{\varphi}{2}+\tan\frac{\psi}{2}\right)-1. \tag{8}$$

In addition

$$\Gamma=\frac{[1-\tan(\varphi/2)]^2}{2\tan(\varphi/2)}=(1+\tan^2\gamma)^{1/2}-1, \tag{9}$$

where $\gamma=90^\circ-\varphi=\psi-90^\circ$ is the angle change between the initially orthogonal diagonals of the square produced by the distortional (shear) deformation (Fig. 2b). Its tangent is

$$\tan\gamma=\frac{1-\tan^2(\varphi/2)}{2\tan(\varphi/2)}=\frac{1}{2}\left(\frac{\lambda_1}{\lambda_2}-\frac{\lambda_2}{\lambda_1}\right), \tag{10}$$

which is a commonly used measure of finite shear strain in a simple shear test. In particular, the amount of the deviatoric portion of the strain $\mathbf{e}_d$ is $e'_d=(\tan\gamma)/2$.

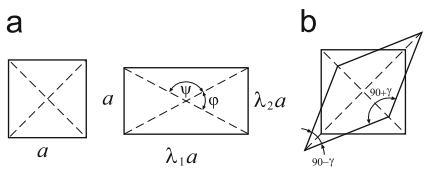

Fig. 2. (a) The angles φ and ψ between the diagonals of the membrane element in its deformed state, under stretch ratios λ_1 and λ_2, used to give the geometric interpretation of Γ. (b) The angle change γ due to shearing of a membrane element, with the stretch ratios λ_1 and $\lambda_2=1/\lambda_1$ along the two diagonals of the element.

3. Kinetics of deformation

If $\phi=\phi(\lambda_1,\lambda_2)$ is the strain energy per unit initial area, the Cauchy stress components are

$$\sigma_1=\frac{1}{\lambda_2}\frac{\partial\phi}{\partial\lambda_1},\quad \sigma_2=\frac{1}{\lambda_1}\frac{\partial\phi}{\partial\lambda_2}. \tag{11}$$

The strain energy of an isotropic membrane must be a symmetric function of λ_1 and λ_2. Evans and Skalak (1980) proposed that $\phi=\phi(\zeta,\Gamma)$, where

$$\zeta=\lambda_1\lambda_2-1,\quad \Gamma=\frac{1}{2}\left(\frac{\lambda_1}{\lambda_2}+\frac{\lambda_2}{\lambda_1}\right)-1, \tag{12}$$

so that in the undeformed configuration $\zeta=\Gamma=0$. As discussed earlier, $\zeta=\mathrm{tr}\,\mathbf{E}_a$ is the area change per unit undeformed area, while $\Gamma=\mathrm{tr}\,\mathbf{E}_d$ is a measure of the distortional deformation. Consistent with the introduced multiplicative decomposition of the deformation gradient, the strain energy is decomposed as $\phi=\phi_a(\zeta)+\phi_d(\Gamma)$, where ϕ_a represents the strain energy due to the area change, and ϕ_d due to distortional deformation. In this case, from (11) there follows:

$$\sigma_{1,2}=\sigma_a\pm\frac{1}{\lambda_a^2}\sigma_d, \tag{13}$$

where

$$\sigma_a=\frac{d\phi_a}{d\zeta},\quad \sigma_d=\frac{d\phi_d}{d\Gamma}\tan\gamma. \tag{14}$$

A simple model of nonlinear elastic membrane is obtained if it is assumed that $\phi_a=\kappa\zeta^2/2$ and $\phi_d=\mu\Gamma$, so that

$$\phi=\frac{1}{2}\kappa(\lambda_1\lambda_2-1)^2+\mu\left[\frac{1}{2}\left(\frac{\lambda_1}{\lambda_2}+\frac{\lambda_2}{\lambda_1}\right)-1\right], \tag{15}$$

where κ and μ are the areal (bulk) modulus and the shear modulus of the membrane, respectively. For example, in the red blood cell, the areal modulus of the membrane is controlled mostly by the phospholipidic bilayer, while the shear modulus is determined by the elastic properties of the cytoskeleton, a network of spectrin strands bound to the bilayer. The strain energy representation (15) was first proposed by Evans and Skalak (1980). The corresponding stresses are

$$\sigma_{1,2}=\kappa(\lambda_1\lambda_2-1)\pm\tfrac{1}{2}\mu\left(\lambda_2^{-2}-\lambda_1^{-2}\right). \tag{16}$$

3.1. Isoareal membranes

If the membrane is infinitely stiff to the area change,[2] there is a deformation constraint $\lambda_1\lambda_2-1=0$. In this case, one can introduce the strain energy function $\Phi=\phi(\lambda_1,\lambda_2)-p_0(\lambda_1\lambda_2-1)$, such that $\lambda_2\sigma_1=\partial\Phi/\partial\lambda_1$ and $\lambda_1\sigma_2=\partial\Phi/\partial\lambda_2$. This gives

$$\sigma_1=\lambda_1\frac{\partial\phi}{\partial\lambda_1}-p_0,\quad \sigma_2=\lambda_2\frac{\partial\phi}{\partial\lambda_2}-p_0, \tag{17}$$

where $p_0=p_0(x_1,x_2)$ is determined by solving a specific boundary-value problem under the consideration. Furthermore, since $\lambda_2=1/\lambda_1$, from (17) we obtain

$$\sigma_1+\sigma_2=-2p_0,\quad \sigma_1-\sigma_2=\lambda_1\frac{d\phi}{d\lambda_1}. \tag{18}$$

By taking the strain energy to be $\phi=\phi_d=\mu\Gamma$, this becomes

$$\sigma_1+\sigma_2=-2p_0,\quad \sigma_1-\sigma_2=\mu\left(\lambda_1^2-\lambda_1^{-2}\right). \tag{19}$$

In the case of small deformations of an isoareal membrane ($\varepsilon_1+\varepsilon_2=0$), the strain energy is $\phi=2\mu\varepsilon_1^2$. The strain components are $\varepsilon_{1,2}=\pm(\sigma_1-\sigma_2)/4\mu$, with the corresponding stresses $\sigma_{1,2}=-p_0\pm2\mu\varepsilon_1$, where p_0 is an arbitrary isotropic tension. The corresponding modulus of elasticity and the coefficient of lateral contraction are $E=4\mu$ and $\nu=1$.

4. Radial stretching of a hollow circular membrane

The red blood cell membrane is a composite structure consisting of an outer phospholipid bilayer, transmembrane proteins, and a network of spectrin molecules attached to the inner cytoplasmic side of the cell. Spectrin is a long filamentous protein, which is cross-linked at junctional complexes containing actin. The transmembrane proteins are tethered to spectrin by ankyrin, which is anchored in the membrane by a covalently bound palmitoyl side chain (Nelson

[2] For example, the shear modulus of the red blood cell is estimated to be in the range 5–20 μN/m, while the areal modulus is in the order 10^3–10^4 higher than that (Fung, 1993; Dao et al., 2003).

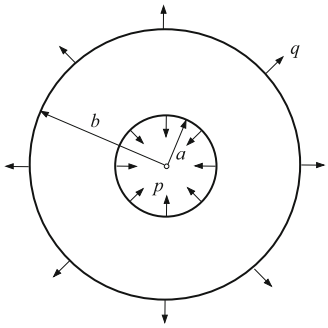

Fig. 3. The inner and outer deformed radii of a hollow membrane are a and b, while the corresponding tensions at two boundaries are p and q.

and Cox, 2005). The areal modulus of the cell membrane is controlled mostly by the phospholipidic bilayer, while the shear modulus is determined by the elastic properties of the cytoskeleton (Hansen et al., 1996). The viscous properties of the cell are due to glycoproteins, lipid rafts, integral and peripheral membrane proteins, and transmembrane cholesterol (Berk et al., 1989; Dao et al., 2003; Lubarda and Marzani, 2009). More involved cell models would incorporate active topological remodeling (dynamic reorganization) of spectrin network (noninert cytoskeleton), due to mechanical, thermal, or chemical driving forces, which results in evolving mechanical properties during large deformation of the red blood cell (Li et al., 2007). For example, it was recently proposed that a metabolic remodeling due to adenosine 5′-triphosphate (ATP) is manifested by association and disassociation of spectrin filaments within the network, or between the cytoskeleton and the lipid membrane, the dissociated filaments spending a longer time disconnected when the network is stretched (Gov, 2007; Park et al., 2010).

The mechanical characterization of the red blood cell is commonly achieved by the micropipette aspiration technique (Evans and Skalak, 1980; Fung, 1993), in which a suction pressure causes the cell to be drawn into a glass tube. If Δp is the pressure difference between the cell and the pipette of inner radius a (suction pressure), the longitudinal stress (per unit length) in the cylindrical portion of the membrane drawn into the pipette is[3] $p = a\Delta p/2$. Assuming that the membrane slides smoothly (freely) at the tip of a small caliber pipette applied to a relatively flat region of the cell membrane, the tension over the inner boundary of the horizontal flat portion of the membrane is also equal to p. With this as a motivation, we consider a hollow circular membrane under internal tension p and external tension q, which accommodates for the pressure difference across the membrane of the undeformed cell. The inner and outer radii of the membrane in its initial, undeformed configuration are a_0 and b_0, while a and b are the radii in the deformed configuration (Fig. 3). The initial radius r_0 at an arbitrary point of the membrane becomes $r=r(r_0)$. The corresponding principal stretches are $\lambda_r = \mathrm{d}r/\mathrm{d}r_0$ and $\lambda_\theta = r/r_0$. It is assumed that the membrane is infinitely stiff to its area change, so that the constraint $\lambda_r\lambda_\theta = 1$ holds, which gives $r\,\mathrm{d}r = r_0\,\mathrm{d}r_0$, i.e., $r^2 = r_0^2 + C$, where C is a constant to be determined from the boundary conditions.[4]

Denoting by σ_r and σ_θ the radial and circumferential stress components, the equilibrium equation, in the absence of body force, is

$$r\frac{\mathrm{d}\sigma_r}{\mathrm{d}r} + \sigma_r - \sigma_\theta = 0. \tag{20}$$

In view of the constitutive equations (19) for an isoareal membrane, the stress difference is $\sigma_r - \sigma_\theta = \mu(\lambda_\theta^{-2} - \lambda_\theta^2)$. Since $\mathrm{d}r = r_0\,\mathrm{d}\lambda_\theta + \lambda_\theta\,\mathrm{d}r_0$ and $\mathrm{d}r_0 = \lambda_\theta\,\mathrm{d}r$, the differential equation (20) becomes

$$\frac{\mathrm{d}\sigma_r}{\mathrm{d}\lambda_\theta} + \mu\left(\frac{1}{\lambda_\theta} + \frac{1}{\lambda_\theta^3}\right) = 0, \tag{21}$$

which has the solution

$$\sigma_r = \frac{1}{2}\mu\left(\frac{1}{\lambda_\theta^2} - \ln\lambda_\theta^2\right) + D = \frac{1}{2}\mu\left(\frac{r_0^2}{r^2} - \ln\frac{r^2}{r_0^2}\right) + D, \tag{22}$$

where D is an integration constant. The expression (22) can be conveniently expressed in terms of r_0 as

$$\sigma_r = \frac{1}{2}\mu\left[\frac{1}{1 + C/r_0^2} - \ln\left(1 + \frac{C}{r_0^2}\right)\right] + D. \tag{23}$$

[3] If the magnitude of the suction pressure is 50 Pa, and with the radius of the pipette typically about 1 μm, the magnitude of p is 25 μN/m, which is about twice the value of the shear modulus, taken to be in the middle of its estimated range 5–20 μN/m.

[4] Beginning with the early work by Rivlin and Thomas (1951), there have been numerous analytical and numerical studies of the stress and deformation fields in hollow membranes or sheets made of highly elastic materials, described by different nonlinear constitutive models; e.g., Green and Adkins (1970), Ogden (1984), Haughton (1998), and the references cited therein.

The corresponding hoop stress follows from (20), and is

$$\sigma_\theta = \frac{1}{2}\mu\left[2\left(1+\frac{C}{r_0^2}\right)-\frac{1}{1+C/r_0^2}-\ln\left(1+\frac{C}{r_0^2}\right)\right]+D. \tag{24}$$

The two boundary conditions needed to specify the constants C and D, $\sigma_r(a_0)=p$ and $\sigma_r(b_0)=q$, give

$$\frac{1}{2}\mu\left[\frac{1}{1+x}-\ln(1+x)\right]+D=p, \tag{25}$$

$$\frac{1}{2}\mu\left[\frac{1}{1+x/k^2}-\ln\left(1+\frac{x}{k^2}\right)\right]+D=q, \tag{26}$$

where $k=b_0/a_0>1$ and $x=C/a_0^2>-1$. The lower bound on x is set to prevent the negative argument in the logarithmic function appearing in (25). The subtraction of (26) from (25) gives a nonlinear equation for x:

$$\frac{1}{2}\left(\frac{1}{1+x/k^2}-\frac{1}{1+x}-\ln\frac{1+x/k^2}{1+x}\right)=\frac{q-p}{\mu}. \tag{27}$$

This equation is solved numerically, and its solution is plotted in Fig. 4 *vs.* the loading parameter $(q-p)/\mu$, for various values of the ratio k. Having x so determined, the constant D follows from (25). The radial displacement is $u(r_0)=r-r_0=(r_0^2+xa_0^2)^{1/2}-r_0$.

The presence of the loading parameter $(q-p)$ in (27) can be explained by noting that the loading (p,q) can be decomposed into the loading $(q-p)$ over the external boundary, and the tension p over both boundaries. Only the $(q-p)$ portion of the loading causes the deformation of an isoareal membrane. It is important to observe that the tension applied over the outer boundary of a hollow membrane gives rise to a tensile hoop stress in the membrane, while the tension applied over the inner boundary induces a compressive hoop stress in the membrane. In the later case, a superposition of an appropriate tension at both boundaries can bring the membrane to an overall tensile state of stress.

For example, if $b_0=3a_0$, $p=0$, and $q=0.75\mu$, we obtain $x=2.447$ (i.e., $C=2.477a_0^2$ and $D=0.4737\mu$). The variations of the corresponding radial and hoop stresses from the inner to the outer boundary of the membrane are shown in Fig. 5a. The plots of $u(r_0)/r_0=[1+x(a_0/r_0)^2]^{1/2}-1$ *vs.* r_0/a_0, for several values of the applied tension q, under $p=0$ and for $k=3$, are shown in Fig. 5b. This type of plots was used by Rivlin and Thomas (1951) to compare their nonlinear rubber model with the experimental results.

4.1. Stress concentration factor

The maximum shear stress at the radius r_0, along the $\pm 45^\circ$ directions relative to the radial direction, is $\tau_{\max}(r_0)=(\sigma_\theta-\sigma_r)/2$. The maximum shear stress at the inner boundary of the membrane and the hoop stress there are

$$\tau_{\max}(a_0)=\frac{1}{2}\mu x\frac{2+x}{1+x}, \quad \sigma_\theta(a_0)=p+2\tau_{\max}(a_0). \tag{28}$$

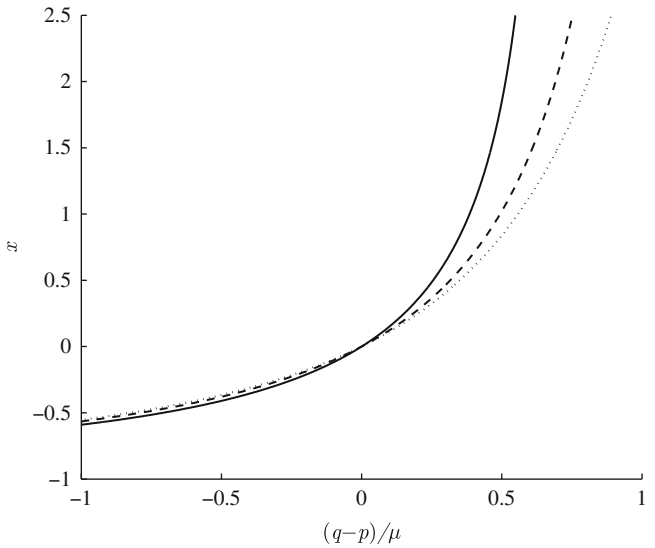

Fig. 4. The plots of x *vs.* $(q-p)/\mu$ according to (27). The solid curve is for $k=5$, the dashed curve is for $k=3$, and the dotted curve is for $k=2$.

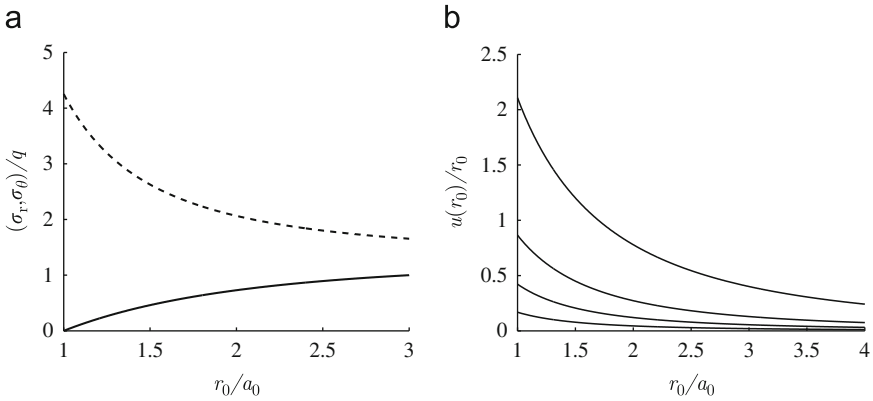

Fig. 5. (a) The variations of the radial (solid curve) and hoop (dashed curve) stresses, normalized by q, along the radius in the case k=3, p=0, and $q=0.75\mu$. (b) The variation of the displacement $u(r_0)/r_0$ with r_0/a_0 corresponding to the tension q of amount 0.25μ (lower-most curve), 0.5μ, 0.75μ, and μ (upper-most curve).

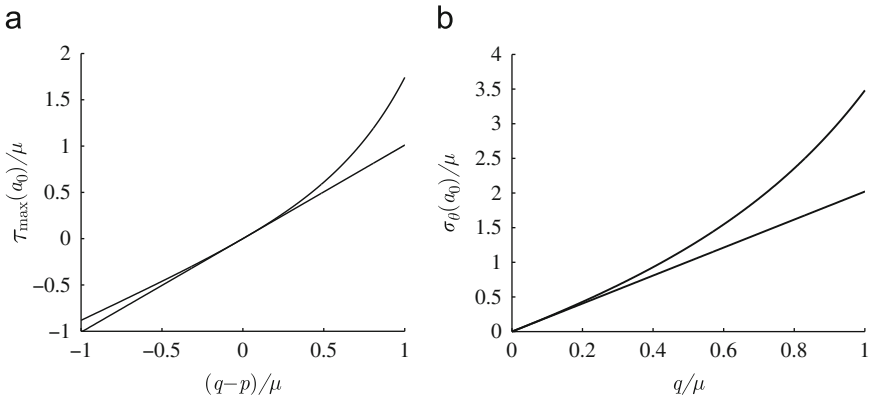

Fig. 6. (a) The shear stress $\tau_{max}(a_0)$ *vs.* the loading parameter $(q-p)$ in the case k=10, according to (31). The straight line corresponds to linear theory. (b) The hoop stress *vs.* the applied tension q in the case p=0 and k=10. The stress concentration factor $\sigma_\theta(a_0)/q$ increases with q, whereas the linear theory predicts the constant value of 2 (the slope of the straight line).

The plot of $\tau_{max}(a_0)$ *vs.* the loading parameter $(q-p)$, in the case k=10, is shown in Fig. 6a. The straight line in this figure corresponds to linear theory. The amplification of the stress concentration factor due to nonlinearity is more pronounced for positive values of the loading parameter.

The increase of the stress concentration factor for the hoop stress with the increasing tension q, under p=0, is shown in Fig. 6b. The stress concentration factor $\sigma_\theta(a_0)/q$ increases with q, being greater than the linear theory prediction of 2. For example, if $q=0.5\mu$, the stress concentration factor is equal to 2.438, while for $q=\mu$ it is 3.479.

4.2. Tension boundary

For negative values of $(q-p)$ in Fig. 6a, the absence of the compressive hoop stress in the membrane needs to be verified, because the tension p at the inner boundary causes the compressive hoop stress, which must be exceeded by the tensile hoop stress due to tension q applied at the outer boundary of the membrane. In other words, the negative values of $(q-p)$ give rise to compressive hoop stress at the inner boundary, which must be exceeded by the tensile hoop stress (p) due to tension p applied at both boundaries, to avoid the net compression in the hoop direction. Otherwise, in the absence of compressive strength and buckling resistance of the membrane, the membrane wrinkling would take place. In order that tension prevails throughout the membrane, we require that $\sigma_\theta(a_0)\geq 0$, which specifies the maximum applied tension p at the inner boundary relative to applied tension q at the outer boundary. Thus, from (28), $p\geq p_c$, where

$$p_c=-\mu x\frac{2+x}{1+x}. \tag{29}$$

The tensile boundary shown in Fig. 7 is obtained by calculating, for each $x>-1$, the critical value of p_c from (29), and (q_c-p_c), and thus q_c, from (27). The three curves shown in Fig. 7 correspond to k=2,3,10. In the loading range (p,q) above the tension boundary (p_c,q_c), tensile stresses prevail throughout the membrane; in the loading range below the tension

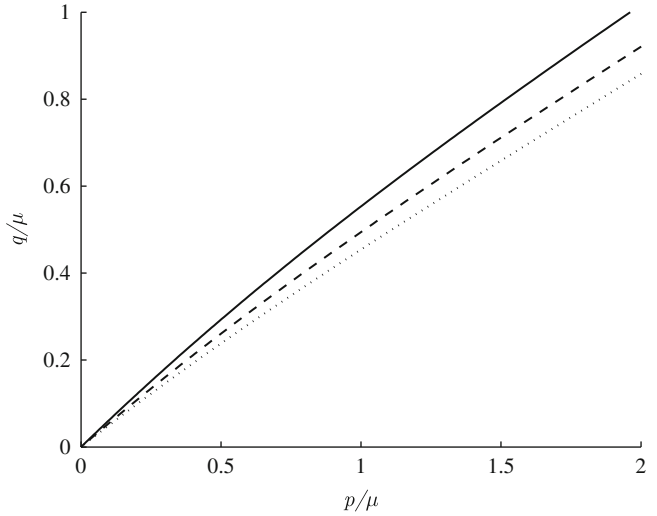

Fig. 7. The tension boundary corresponding to $\sigma_\theta(a_0)=0$. The tensile stresses prevail throughout the membrane for the loading pairs (p,q) which lie above the plotted curves. The solid curve is for $k=2$, the dashed curve is for $k=3$, and the dotted curve is for $k=10$.

boundary, the hoop stress becomes compressive near the inner portion of the membrane, in spite of tensile radial stresses at both boundaries.

If $q=0$, any level of applied tension p at the inner boundary will induce a compressive circumferential stress, and, in the absence of buckling strength, cause immediate wrinkling of the membrane. In view of this observation, we note that the well-known analysis of the micropipette aspiration test by Evans and Skalak (1980, pp. 160–166), which assumes $q=0$ at the remote boundary and which does not account for this wrinkling, should be reexamined.

4.3. Tension field

A simplified analytical study of the membrane response for the loading below the tension boundary can be performed by adopting the so-called tension field theory (Reissner, 1938; Pipkin, 1986; Steigmann, 1990). In this theory, the details of wrinkling are ignored by assuming that wrinkles are continuously distributed and infinitesimal. Such analysis has been used to study various thin membrane problems, including bending of a stretched rectangular membrane and twisting of a hollow stretched membrane (Miller et al., 1985), combined stretching and shearing of a rectangular strip, with and without a hole (Haseganu and Steigmann, 1994), and wrinkling of annular disks made of Varga materials subjected to radial displacements (Haughton and McKay, 1995; Haughton, 2001).

If the loading (p,q) lies below the tension boundary in Fig. 7, the inner portion of the membrane $(a\le r\le\rho)$ supports only the radial stress, while the circumferential stress is identically equal to zero $(\sigma_\theta=0)$. The extent of infinitesimal wrinkling ρ will be determined in the sequel. Thus, the equilibrium equation in this portion of the membrane is

$$r\frac{\mathrm{d}\sigma_r}{\mathrm{d}r}+\sigma_r=0,\quad a\le r\le\rho, \tag{30}$$

with the solution $\sigma_r=pa/r=t\rho/r$, where $t=\sigma_r(\rho)$ is the radial stress at the boundary between the tension region and the outside portion of the membrane.

Within the tension field region, the wrinkles are assumed to be continuously distributed and infinitesimal. As a consequence of wrinkling, which takes place in circumferential direction, the effective area of the membrane within the plane of the membrane will decrease and the local area decrease is more pronounced in the region of more intense wrinkling.[5] Consequently, we shall model the wrinkled membrane in the tension region as a flat membrane carrying radial tension but no circumferential stress, capable of decreasing its effective flat area. Therefore

$$\sigma_r=\frac{1}{\lambda_\theta}\frac{\partial\phi_*}{\partial\lambda_r},\quad \sigma_\theta=\frac{1}{\lambda_r}\frac{\partial\phi_*}{\partial\lambda_\theta}=0\quad (a\le r\le\rho), \tag{31}$$

where ϕ_* is the strain energy density (per unit initial area) of the wrinkled membrane. The vanishing of the circumferential stress implies that $\phi_*=\phi_*(\lambda_r)$. Since at the boundary of the wrinkled region $(r=\rho)$, the radial stress is $\sigma_r=\mu(\lambda_r^2-\lambda_r^{-2})$, and

[5] Another type of wrinkling of the erythrocyte membrane, not considered here, is associated with thermal undulations and nonequilibrium dynamic fluctuations—flickering, which is enhanced by local breaking and reforming of the spectrin network (Park et al., 2010).

since there $\lambda_\theta = \lambda_r^{-1}$, the following representation of the strain energy density suggests itself

$$\phi_* = \frac{1}{2}\mu(\lambda_r^2 + \lambda_r^{-2} - 2), \quad \lambda_r \geq 1. \tag{32}$$

The corresponding radial stress is

$$\sigma_r = \mu \frac{1}{\lambda_r \lambda_\theta}(\lambda_r^2 - \lambda_r^{-2}), \tag{33}$$

i.e.,

$$\sigma_r = \mu \frac{r_0}{r}\frac{\mathrm{d}r_0}{\mathrm{d}r}\left[\left(\frac{\mathrm{d}r}{\mathrm{d}r_0}\right)^2 - \left(\frac{\mathrm{d}r_0}{\mathrm{d}r}\right)^2\right]. \tag{34}$$

In the outer portion of the membrane ($\rho \leq r \leq b$), both radial and circumferential tensile stresses exist, governed by the expressions (23) and (24). Denoting the radial stress at $r = \rho$ by t, the boundary conditions $\sigma_r(\rho) = t$ and $\sigma_r(b) = q$ give

$$\frac{1}{2}\mu\left[\frac{1}{1+x} - \ln(1+x)\right] + D = t, \tag{35}$$

$$\frac{1}{2}\mu\left[\frac{1}{1+x/k^2} - \ln\left(1 + \frac{x}{k^2}\right)\right] + D = q, \tag{36}$$

where $k = b_0/\rho_0$, and

$$x = \frac{C}{\rho_0^2} > -1, \quad C = r^2 - r_0^2, \quad r_0 \geq \rho_0. \tag{37}$$

The subtraction of (35) from (36) gives

$$\frac{1}{2}\left(\frac{1}{1+x/k^2} - \frac{1}{1+x} - \ln\frac{1+x/k^2}{1+x}\right) = \frac{q-t}{\mu}. \tag{38}$$

But the circumferential stress at $r = \rho$ is equal to zero, so that

$$\frac{1}{2}\mu\left[2(1+x) - \frac{1}{1+x} - \ln(1+x)\right] + D = 0. \tag{39}$$

When this is combined with (35) to eliminate D, the tension t can be expressed as

$$t = -\mu\left(1 + x - \frac{1}{1+x}\right). \tag{40}$$

The substitution of (40) into (38) yields

$$\frac{1}{2}\left[\frac{1}{1+x/k^2} + \frac{1}{1+x} - 2(1+x) - \ln\frac{1+x/k^2}{1+x}\right] = \frac{q}{\mu}. \tag{41}$$

For a given q/μ and assumed value of $\rho_0 > a_0$, this equation can be solved for x.

Having x so determined, the tension t follows from (40), while $\rho = \rho_0(1+x)^{1/2}$. The radial stress in the tension region can therefore be expressed as

$$\sigma_r = \mu\frac{\alpha\rho_0}{r}, \quad \alpha = (1+x)^{1/2}\left(\frac{1}{1+x} - 1 - x\right). \tag{42}$$

It remains to determine the tension p associated with the assumed value of ρ_0 and calculated x, and to determine the variation of the displacement within the tension field region. Both follow by determining the variation $r = r(r_0)$ within the tension field region. This is accomplished by equating the expressions (34) and (42), which yields a differential equation

$$\left(\frac{\mathrm{d}r}{\mathrm{d}r_0}\right)^4 - \frac{\alpha\rho_0}{r_0}\left(\frac{\mathrm{d}r}{\mathrm{d}r_0}\right)^3 - 1 = 0, \quad a_0 \leq r_0 \leq \rho_0. \tag{43}$$

This quartic equation for $\mathrm{d}r/\mathrm{d}r_0$ has only one real and positive root, which is

$$\frac{\mathrm{d}r}{\mathrm{d}r_0} = \frac{\alpha\rho_0}{4r_0} + \frac{1}{2}(f+g), \tag{44}$$

where the functions $f = f(r_0)$ and $g = g(r_0)$ are

$$f = \left(\frac{\alpha^2\rho_0^2}{4r_0^2} + z\right)^{1/2}, \quad g = \left(\frac{\alpha^2\rho_0^2}{2r_0^2} - z + \frac{\alpha^3\rho_0^3}{4r_0^3 f}\right)^{1/2}. \tag{45}$$

The function $z=z(r_0)$ is defined by

$$z=\left(-\frac{\alpha^2\rho_0^2}{2r_0^2}+w^{1/2}\right)^{1/3}-\left(\frac{\alpha^2\rho_0^2}{2r_0^2}+w^{1/2}\right)^{1/3}, \quad w=\frac{64}{27}+\frac{\alpha^4\rho_0^4}{4r_0^4}. \tag{46}$$

The first order quasi-linear differential equation (44), with the boundary condition $r(\rho_0)=\rho_0(1+x)^{1/2}$, can be solved numerically by using the ode45 solver. The displacement within the tension field is then $u(r_0)=r(r_0)-r_0$, while the corresponding tension at the inner boundary of the membrane is, from (42), $p=\mu\alpha\rho_0/a$, where $a=r(a_0)$.

The variations of σ_r and σ_θ with r_0, in the case $\rho_0=1.5a_0$ and $q=0.5\mu$, so that $x=-0.3518$ and $p=1.968\mu$, are shown in Fig. 8a. The dotted curves correspond to the analysis based on the original theory, without the correction based on the tension field analysis. Due to the stress redistribution by the inclusion of the tension field, the value of ρ at which the circumferential stress vanishes is greater than that predicted by the analysis without the tension field correction. Note the continuity of the gradient of the radial stress at $r=\rho$, which follows from (30) and the continuity of the radial stress itself. The effect of wrinkling on both radial and circumferential stresses increases with the increase of ρ_0. Fig. 8b shows the variation of the displacement $u=u(r_0)$. The end displacements are $u(a_0)=-0.451a_0$ and $u(b_0)=-0.135a_0$. The corresponding values without the tension field correction are $u(a_0)=-0.422a_0$ and $u(b_0)=-0.113a_0$, which is in magnitude substantially less inward than the displacements based on the tension field theory. This difference may be of importance for the interpretation of results obtained from the red blood aspiration tests in the pressure range for which the wrinkling of the membrane may take place.

The wrinkling between a_0 and ρ_0 has absorbed the membrane area of the amount $\Delta A_w=\pi(\rho_0^2-a_0^2)-\pi(\rho^2-a^2)=\pi[r^2(a_0)-a_0^2-x\rho_0^2]$. For example, if $\rho_0=1.5a_0$, this gives a 7.43% area reduction relative to the initial area $\pi(\rho_0^2-a_0^2)$ of the wrinkled region. Fig. 9a shows the variation of the specific area decrease $\Delta(dA)/dA=1-\lambda_r\lambda_\theta$ along $a_0\le r_0\le\rho_0$. The corresponding effective area modulus of the wrinkled membrane is negative because, due to its wrinkling, the membrane area decreases in spite of being subjected to tensile radial stress.

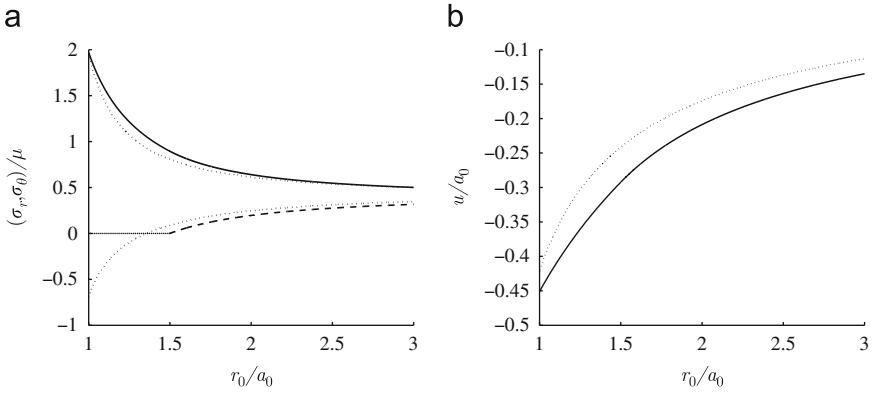

Fig. 8. (a) The radial stress distribution with the tension field correction (solid curve) and without it (nearby dotted curve). The dashed curve and its nearby dotted curve are the corresponding variations of the hoop stress. The curves are obtained for the loading $p=1.968\mu$ and $q=0.5\mu$, while $b_0=3a_0$. The tension field ($\sigma_\theta=0$) extends to $\rho_0=1.5a_0$ and $t=\sigma_r(\rho_0)=0.894\mu$. (b) The displacement variation with the tension field correction (solid curve) and without it (dashed curve), for the same loading as in part (a).

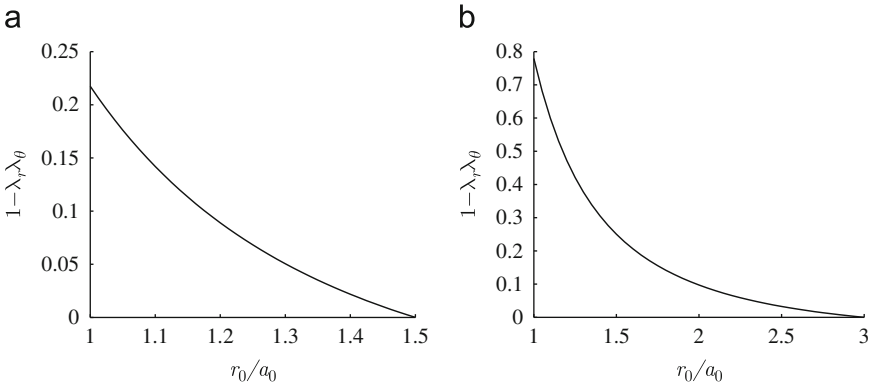

Fig. 9. (a) The variation of the specific area decrease $1-\lambda_r\lambda_\theta$ along r_0 at: (a) $\rho_0=1.5a_0$, and (b) the limiting state $\rho_0=b_0$. The plots are for $q=0.5\mu$ and $b_0=3a_0$.

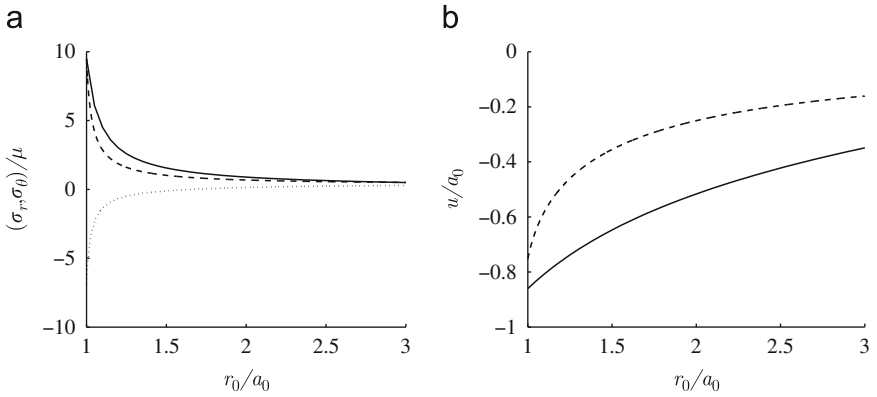

Fig. 10. (a) The radial stress distribution in the limiting state $\rho_0 = b_0$ (solid curve). The dashed curve is the radial stress without the tension field correction. The corresponding hoop stress in the latter case is represented by the dotted curve. The results are for $b_0 = 3a_0$, $p = 9.488\mu$ and $q = 0.5\mu$. (b) The displacement variation with the tension field correction (solid curve) and without it (dashed curve), for the same loading as in part (a).

4.4. Limit boundary

The maximum extent of the tension field is $\rho_0 = b_0$, in which case the entire membrane is infinitesimally wrinkled and under radial tension $\sigma_r = pa/r = qb/r$. In the limit as $\rho_0 \to b_0$, the expressions (40) and (41) both give

$$1+x-\frac{1}{1+x} = -\frac{q}{\mu}. \tag{47}$$

For a given q, this can be solved for $(1+x)$ to obtain

$$1+x = \frac{1}{2}\left[-\frac{q}{\mu}+\sqrt{\left(\frac{q}{\mu}\right)^2+4}\right]. \tag{48}$$

The parameter α in (42) reduces to $\alpha = (1+x)^{1/2}q\mu$. With this value of α, and with $\rho_0 = b_0$ in (45) and (46), the differential equation (44) can be solved numerically, subject to the boundary condition $r(b_0) = b = b_0(1+x)^{1/2}$. When this is done, we obtain the variation $r = r(r_0)$ and thus the displacement field $u(r_0) = r(r_0) - r_0$. The radial stress $\sigma_r = qb/r$ becomes

$$\sigma_r = \frac{b_0(1+x)^{1/2}}{r(r_0)}q, \quad a_0 \le r_0 \le b_0. \tag{49}$$

Fig. 10a shows the variation of the radial stress in the case $q = 0.5\mu$ (giving $x = -0.2192$). The tension on the internal boundary of the membrane is $p = 9.488\mu$. The hoop stress is zero everywhere in the membrane. Without the tension field correction, the hoop stress is as shown by the dotted line in Fig. 10a, with $\sigma_\theta(a_0) = -6.845\mu$ and $\sigma_\theta(b_0) = 0.285\mu$. The plot of $u = u(r_0)$ is shown in Fig. 10b. The end displacements are $u(a_0) = -0.86a_0$ and $u(b_0) = -0.349a_0$. The corresponding values without the tension field correction are $u(a_0) = -0.753a_0$ and $u(b_0) = -0.161a_0$, which is substantially less inward than the displacements based on the tension field theory. The magnitude of the maximum difference of the displacement predicted by two theories is $0.293a_0$, which occurs at $r_0 = 1.474a_0$. The infinitesimal wrinkling of the membrane has absorbed 12.41% of the membrane area. Fig. 9b shows the corresponding variation of the specific area decrease $1-\lambda_r\lambda_\theta$ along the radius of the membrane.

The limit boundary $q = q(p)$, specifying the loading pairs (p,q) for which the infinitesimal wrinkling has spread throughout the entire membrane is obtained by repeating the above calculations for each value of $q \ge 0$. The lower curve in Fig. 11a is the resulting limit boundary, in the case $b_0 = 3a_0$. The upper curve represents the tension boundary. The loading pairs (p,q) below the limit boundary cannot be supported by the membrane without its unstable (localized) wrinkling.[6] The limit and tension boundaries are closer to each other smaller the value of the ratio b_0/a_0. This is illustrated in Fig. 11b. For each b_0/a_0, there is a saturation value of $q = \hat{q}$ to which the limit boundary asymptotically approaches as p increases indefinitely. If $b_0 = 3a_0$, the limit boundary approaches $\hat{q} = 0.5725\mu$ as p increases indefinitely. If $q > \hat{q}$, the membrane will not wrinkle unstably regardless of how large is the applied tension p at the inner boundary, provided that no rupture intervenes in the limiting process. In fact, if $q > \hat{q}$ and $p \to \infty$, from (49) it follows that the radius of the hole $a = r(a_0)$ shrinks to zero.

For example, if $q = 0.75\mu$ and $b_0 = 3a_0$, then $x = -0.4346$ and the limiting extent of the tension field is $\rho_0 = 1.96a_0$, the radial tension at $r_0 = \rho_0$ being $t = 1.203\mu$, as calculated from (40). The plot of ρ_0/a_0 versus p/μ in this case is shown in

[6] The analysis of unstable wrinkling and the determination of the shape and distribution of finite wrinkles is beyond the membrane theory, and requires the incorporation of the bending stiffness of the membrane (Helfrich, 1973; Steigmann, 1999). See also Mansfield (1960).

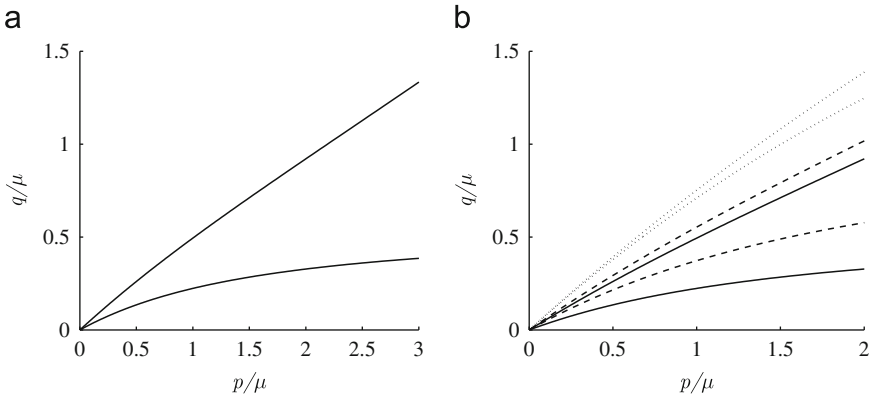

Fig. 11. (a) The tensile stresses prevail throughout the membrane for the loading pairs (p,q) which lie above the tension boundary (upper curve). The loading pairs (p,q) below the limit boundary (lower curve) cannot be supported by the membrane without its unstable wrinkling. The plots are for $b_0=3a_0$, in which case the limit boundary approaches $\hat{q}=0.5725\mu$ as p increases indefinitely. (b) The limit and tension boundaries are closer to each other smaller the value of the ratio b_0/a_0. The solid curves are for $b_0/a_0=3$, the dashed curves are for $b_0/a_0=2$, and the dotted curves are for $b_0/a_0=1.25$.

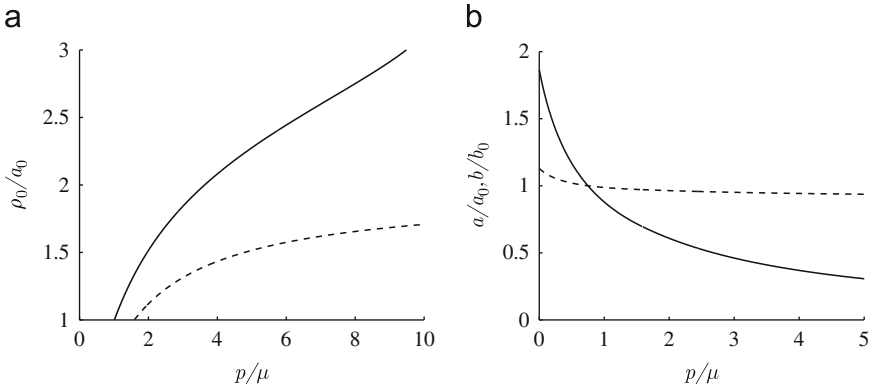

Fig. 12. (a) The increase of the extent of infinitesimal wrinkling ρ_0 with the increasing $p>p_c$, at constant $q=0.5\mu$ (solid curve) and $q=0.75\mu$ (dashed curve), when $b_0=3a_0$. The limit boundary ($\rho_0=b_0$) in the former case is reached at $\hat{p}_c=9.488\mu$ The maximum extent of the wrinkling in the latter case, as $p\to\infty$, is $\rho_0^{\max}=1.96a_0$. (b) The variation of the normalized deformed radii a/a_0 (solid curve) and b/b_0 (dashed curve) with the increasing p, at constant $q=0.75\mu$. In the limit as p increases indefinitely, $\rho_0\to1.96a_0$ and $a\to0$.

Fig. 12a. The critical value of p at the tension boundary is $p_c=1.591\mu$, which is calculated from (29) in the case $q=0.75\mu$. The corresponding $x=-0.5177$ was calculated by solving the nonlinear equation obtained by substituting (29) into (27). The variation of the normalized deformed radii a/a_0 and b/b_0 with p is shown in Fig. 12b.

Fig. 12a also shows the variation of $\rho_0=\rho_0(r_0)$ in the case $b_0=3a_0$ and $q=0.5\mu$, as p increases from the value $p_c=1.013\mu$ at the tension boundary (with the corresponding $x=-0.3855$), to $\hat{p}_c=9.488\mu$ at the limit boundary (with the corresponding $x=-0.2192\mu$). The tension field analysis, with continuously distributed infinitesimal wrinkles, does not apply beyond this value of $\hat{p}_c$.

5. Discussion

We have presented in this paper the constitutive analysis of thin biological membranes by using the multiplicative decomposition of the deformation gradient into its areal and distortional parts. Kinematic aspects of the analysis were presented in Section 2, and the kinetic aspects in Section 3. Consistent with the introduced multiplicative decomposition of the deformation gradient, the strain energy was decomposed into contributions from the areal and distortional deformations. The stress response was derived in the general case and in the case of the Evans–Skalak biological membrane model. The solution to the problem of the radial stretching of a hollow circular membrane obeying this constitutive model was derived in Section 4. The stress concentration factor was determined as a function of the relative hole size and the magnitude of the applied tension. Its amplification due to nonlinearity is evaluated. We identify the tension boundary above which no compressive stress appears in the membrane, and the limit boundary below which the membrane cannot support the loading without unstable wrinkling. For the loadings between the tension and the limit boundary, tension field theory is used to derive the stress and displacement fields in the region of continuously distributed infinitesimal wrinkles.

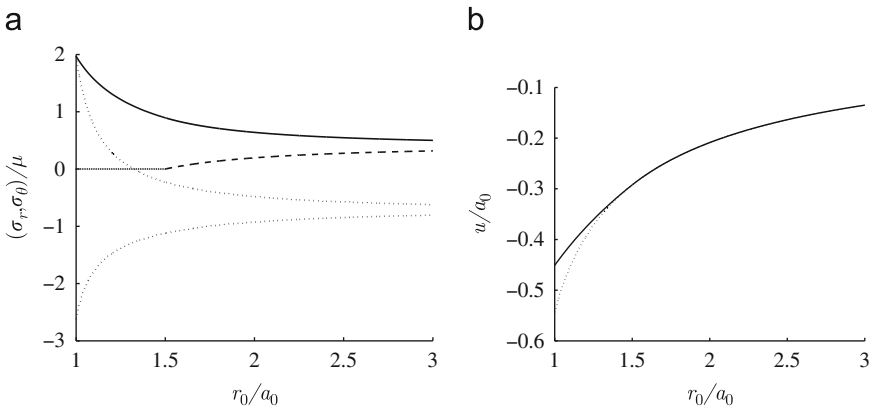

Fig. 13. (a) The radial stress (solid curve) and the hoop stress (dashed curve) in the case of the prescribed loading $p=1.968\mu$ at the inner boundary and the displacement $u_b=-0.135a_0$ at the outer boundary, in the case $b_0=3a_0$. The tension field extends to $\rho_0=1.5a_0$. The dotted curves are the radial and hoop stresses without the tension field correction. (b) The displacement variation for the same loading as in part (a).

The specific form of the strain energy function is used to describe this behavior and to calculate the amount of the membrane area absorbed by infinitesimal wrinkling. The limit boundary is reached when the wrinkles spread throughout the membrane. It is shown that for a sufficiently large tension at the outer boundary, the membrane will not reach the state at the limit boundary no matter how large the applied tension at the inner boundary of the membrane is, provided that no rupture takes place. The limiting extent of the wrinkled zone in such cases is determined.

The presented analysis of the radial stretching of a hollow membrane can be extended to the mixed type boundary conditions, in which the displacement is prescribed on the inner boundary and the traction on the outer boundary, or *vice versa*. The details of the derivation are omitted for brevity; only comments on some of the obtained results are given. The variations of σ_r and σ_θ with r_0, in the case $p=1.968\mu$ and $u_b=-0.135a_0$, so that the tension field extends to $\rho_0=1.5a_0$, are shown in Fig. 13a. The dotted curves correspond to the analysis which does not include the correction based on the tension field. There is a dramatic difference between the stress fields predicted by the two theories. While the tension field theory predicts $q=0.5\mu$, the value $q=-0.621\mu$ is obtained in the theory without the tension field correction. In the latter case, the hoop stress is negative (compressive) throughout the membrane, while $\sigma_\theta(b_0)=0.316\mu$ according to tension field theory. Fig. 13b shows the corresponding variation of the displacement $u=u(r_0)$. Both theories predict the same displacements outside the tension field, because the prescribed displacement u_b uniquely specifies the displacement in an isoareal (unwrinkled) portion of the membrane. The difference in the predicted displacement within the wrinkled region increases toward the hole of the membrane, so that $u(a_0)=-0.451a_0$ according to the tension field theory, while $u(a_0)=-0.543a_0$ without the tension field correction. Physically, the reason for a large difference in the stress field is that the prescribed displacement $u_b=-0.135a_0$, under tensile stress at the inner boundary of amount 1.968μ, is so much inward that it can take place in the membrane with a compressive strength only if accompanied (aided) by the compression of amount 0.621μ at the outer boundary.

Finally, we note that in the case of infinitesimally small strains, the nonlinear equation (27) reduces to a linear equation for x. The tension boundary in the (p,q) plane is a straight line $q=p(1+a^2/b^2)/2$, while the limit boundary is $q=pa/b$. For example, if $q=0$, the membrane cannot support any p without wrinkling, because the positive p-axis is under the limit boundary. On the other hand, if $p=0$, the membrane can support any tension q (before rupture or other tensile failure), because the positive q-axis is above the tension boundary. For a very small hole in a large membrane, the tension boundary approaches the line $q=p/2$, while the limit boundary approaches the horizontal line $q=0$.

Acknowledgment

The conducted research was supported by the Montenegrin Academy of Sciences and Arts. Helpful comments and suggestions by reviewers are also gratefully acknowledged.

References

Berk, D.A., Hochmuth, R.M., Waugh, R.E., 1989. Viscoelastic properties and rheology. In: Agre, P., Parker, J.C. (Eds.), Red Blood Cell Membranes: Structure, Function, Clinical Implications. Marcel Dekker, Inc., New York, pp. 423–454.

Boal, D., 2002. Mechanics of the Cell. Cambridge University Press, New York.

Dao, M., Lim, C.T., Suresh, S., 2003. Mechanics of the human red blood cell deformed by optical tweezers. J. Mech. Phys. Solids 51, 2259–2280.

Dervaux, J., Ciarletta, P., Ben Amar, M., 2009. Morhogenesis of thin hyperelastic plates: a constitutive theory of biological growth in the Föppl–von Karman limit. J. Mech. Phys. Solids 57, 458–471.

Evans, E.A., Skalak, R., 1980. Mechanics and Thermodynamics of Biomembranes. CRC Press, Boca Raton.

Fung, Y.C., 1993. Biomechanics: Mechanical Properties of Living Tissues. Springer, New York.

Garikipati, K., Olberdin, J.E., Narayanan, H., Arruda, E.M., Grosh, K., Calve, S., 2006. Biological remodelling: stationary energy, configurational change, internal variables and dissipation. J. Mech. Phys. Solids 54, 1493–1515.
Gov, N.S., 2007. Active elastic network: cytoskeleton of the red blood cell. Phys. Rev. E 75, 011921-1–011921-6.
Green, A.E., Adkins, J.E., 1970. Large Elastic Deformations. Oxford University Press, Oxford.
Hansen, J.C., Skalak, R., Chien, S., Hoger, A., 1996. An elastic network model based on the structure of the red blood cell membrane skeleton. Biophys. J. 70, 146–166.
Haseganu, E.M., Steigmann, D.J., 1994. Analysis of partly wrinkled membranes by the method of dynamic relaxation. Comput. Mech. 14, 596–614.
Haughton, D.M., 1998. Exact solutions for elastic membrane disks. Math. Mech. Solids 4, 393–410.
Haughton, D.M., 2001. Elastic membranes. In: Fu, Y.B., Ogden, R.W. (Eds.), Nonlinear Elasticity: Theory and Applications. Cambridge University Press, Cambridge, UK, pp. 233–267.
Haughton, D.M., McKay, B.A., 1995. Wrinkling of annular discs subjected to radial displacements. Int. J. Eng. Sci. 33, 335–350.
Helfrich, W., 1973. Elastic properties of lipid bilayers: theory and possible experiments. Z. Naturforsch. 28C, 693–703.
Li, J., Lykotrafitis, G., Dao, M., Suresh, S., 2007. Proc. Nat. Acad. Sci. USA 104, 4937–4942.
Lubarda, V.A., Hoger, A., 2002. On the mechanics of solids with a growing mass. Int. J. Solids Struct. 39, 4627–4664.
Lubarda, V.A., Marzani, A., 2009. Viscoelastic response of thin membranes with application to red blood cells. Acta Mech. 202, 1–16 (with Addendum, Acta Mechanica, in press).
Mansfield, E.H., 1960. On the buckling of an annular plate. Q. J. Mech. Appl. Math. 13, 16–23.
Miller, R.K., Hedgepeth, J.M., Weingarten, V.I., Das, P., Kahyai, S., 1985. Finite element analysis of partly wrinkled membranes. Computers & Structures 20, 631–639.
Nelson, D.L., Cox, M.M., 2005. Lehninger Principles of Biochemistry, fourth ed. W.H. Freeman, New York.
Ogden, R.W., 1984. Non-Linear Elastic Deformations. Ellis Horwood Ltd., Chichester, England (second ed., Dover, 1997).
Park, Y.-K., Best, C.A., Auth, T., Gov, N.S., Safran, S.A., Popescu, G., Suresh, S., Feld, M.S., 2010. Proc. Nat. Acad. Sci. USA 107, 1289–1294.
Pipkin, A.C., 1986. The relaxed energy density for isotropic elastic membranes. IMA J. Appl. Math. 36, 85–99.
Reissner, E., 1938. On tension field theory. In: Proceedings of the Fifth International Congress for Applied Mechanics, pp. 88–92.
Rivlin, R.S., Thomas, A.G., 1951. Large elastic deformations of isotropic materials. VIII. Strain distribution around a hole in a sheet. Philos. Trans. R. Soc. Lond. A 243, 289–298.
Steigmann, D.J., 1990. Tension field theory. Proc R. Soc. Lond. A 429, 141–173.
Steigmann, D.J., 1999. Fluid films with curvature elasticity. Arch. Ration. Mech. Anal. 150, 127–152.
Taber, L.A., 2009. Towards a unified theory for morphomechanics. Philos. Trans. R. Soc. A 367, 3555–3583.